ISSN 0915-633X

NATIONAL INSTITUTE FOR FUSION SCIENCE

Dynamics of the Dust Charging on Electrostatic Waves in a Dusty Plasma with Trapped Electrons

Y.-N. Nejoh

(Received - Sep. 2, 1997)

NIFS-508 Sep.1997

This report was prepared as a preprint of work performed as a collaboration reserch of the National Institute for Fusion Science (NIFS) of Japan. This document is intended for infomation only and for future publication in a journal after some rearrangements of its contents.

Inquiries about copyright and reproduction should be addressed to the Research Information Center, National Institute for Fusion Science, Oroshi-cho, Toki-shi, Gifu-ken 509-02 Japan.

RESEARCH REPORT
NIFS Series

NAGOYA, JAPAN

DYNAMICS OF THE DUST CHARGING ON ELECTROSTATIC WAVES IN A DUSTY PLASMA WITH TRAPPED ELECTRONS

Y-N.Nejoh

Graduate Scool of Engineering and Department of Electronic Engineering, Hachinohe Institute of Technology, Myo-Obiraki, Hachinohe, 031, Japan

Dynamics of the dust charging and the influence of the ion density and temperature on electrostatic nonlinear waves in a dusty plasma having trapped electrons are investigated by numerical calculation. The nonlinear structure of the dust charging is examined, and it is shown that the characteristics of the dust charge number sensitively depend on the plasma potential, Mach number, trapped electron temperature, ion density and temperature. An increase of the ion temperature decreases the dust charging rate and the propagation speed of ion waves. It turns out that a decrease of the trapped electron temperature increases the charging rate of dust grains. It is found that the existence of ion waves sensitively depends on the ion to electron density ratio. New findings of variable-charge dust grain particles, ion density and temperature in a dusty plasma with trapped electrons are predicted.

Key words: nonlinear dust charging, the existence of electrostatic nonlinear waves,
trapped electrons, the effect of the ion to electron density ratio,

I. INTRODUCTION

The increase of recent interest in plasmas containing charged, micrometer-sized dust particles has arisen not only from the increase of observations of such plasmas in space environments such as asteroid zones, cometary tails, planetary rings and magnetospheres, and the lower ionosphere of the Earth[1-4], but also from their presence in laboratory devices[5-7]. In reality, the dust grains have variable-charge and mass due to fragmentation and coalescence. However, in studying collective effects involving charged dust grains in dusty plasmas one generally assumes that the dust particles behave like point charges. Multi-fluid descriptions for collective modes in micro-particle plasmas were presented by several authors. For low frequency nonlinear wave modes, the dust grains can be described as negative ions with large mass and large charge. Ion- and dust-acoustic wave modes in dusty plasmas have been treated by several authors[8-13]. We have suggested that high-speed streaming particles excite various kind of nonlinear waves in space[14-17]. Dust grain particles are charged due to the local electron and ion currents, and its charge varies as a result of the change of the parameters such as the potential, densities, *etc*. Therefore, since the dust charge variation affects the characteristics of the collective motion of the plasma, the effect of variable-charge dust grain particles is of crucial importance in understanding dusty plasma waves. However, not many theoretical works on the effect of variable-charge dust grain particles have been done in dusty plasmas. In particular, the effects of the ion temperature and trapped electrons have not been investigated in dusty plasmas.

The motivation of this articles is as follows. If streaming particles inject in plasmas, we often find that they evolve towards a coherent trapped particle state. This has been confirmed in experiments[18]. The onset of an electron trapping is also seen in the formation of double layers[19] and computer simulation[20]. When the amplitude of nonlinear waves becomes large, some electrons, in general, would be trapped in the electrostatic potential trough of the wave and be carried along with the wave. Electron trapping is essentially a nonlinear phenomenon. There is no doubt that an electron trapping exists in nonlinear wave phenomena. Thus, the inclusion of the effect of trapped electrons is indispensable to considering nonlinear waves. However, theoretical investigations in relation to the trapped electron effect have not been considered in dusty plasmas. Hence, an aim of this article is to show this effect in order to apply this theory to more extensive nonlinear wave phenomena.

In this paper, we focus our attention on electrostatic ion waves in an unmagnetized dusty plasma having trapped electrons and positive ions with finite temperature. It is therefore instructive to examine the effects of the dust charging, ion temperature and trapped electrons in dusty plasmas, which, as pointed out earlier, are observed as components of broad regions of space plasmas, from the lower ionosphere of the Earth to asteroid zones, cometary tails, *etc*. Our plasma model consists of non-Boltzmann distributed electrons with a constant temperature, positive ions with finite temperature, and the negatively charged dust fluid obeying the nonlinear continuity and momentum equations. We derive a nonlinear equation for variable-charge dust particles and the Sagdeev potential of electrostatic nonlinear waves. We show the dependence of the dust grain charging on the electrostatic potential, ion temperature, trapped electrons and Mach number. Our results show the existence of supersonic electrostatic waves and illustrate the dependence of the dust charge number on the parameters such as the potential, Mach number, trapped electrons, ion to electron density ratio and ion temperature.

In Sec. II, we present a new nonlinear equation for variable-charge dust particles and derive the Sagdeev potential from the basic equations. In Sec. III, we show the numerical results of the nonlinear equations obtained in the preceding section. It is shown that the charging effect of the dust grain particles drastically changes due to the several parameters. Section IV is devoted to the concluding discussion.

II. THEORY

We consider a collisionless, unmagnetized three component plasma consisting of non-Boltzmann electrons with a constant temperature T_e, warm ions having a temperature T_i and negatively charged, heavy, dust particles, and assume that low frequency electrostatic waves propagate in this system. The number density of the electron fluid is assumed to be the trapped electron distribution[21],

$$n_e = n_0 K\left[\exp\left(\frac{e\phi}{T_e}\right)\mathrm{erfc}\left(\sqrt{\frac{e\phi}{T_e}}\right) + \sqrt{\frac{T_t}{T_e}}\exp\left(\frac{e\phi}{T_t}\right)\mathrm{erf}\left(\sqrt{\frac{e\phi}{T_t}}\right)\right], \tag{1}$$

where n_e, n_0, e and ϕ are the electron density, background electron density, the magnitude of electron charge and the electrostatic potential. Here, K=1 in the isothermal process, T_e and T_t are the free and trapped electron temperature. It is significant to consider the dependence of the trapped electron density n_e on the electrostatic potential ϕ and free to trapped electron temperature ratio $T_e/T_t(\equiv\beta)$ in the sense that electrostatic waves closely connect with the trapped electron density. The electron density (1) includes the two states of the electron distribution, namely, (i) in the limit of $\beta\to 1$ (T_e=T_t), n_e approaches the Boltzmann distribution, (ii) β=0 means the state for flat-topped distribution. A figure showing n_e vs ϕ for various values of β is shown in an Appendix.

The continuity equation and the equation of motion for ions are described by,

$$\frac{\partial n_i}{\partial t} + \frac{\partial}{\partial x}(n_i v_i) = 0, \tag{2.a}$$

$$\frac{\partial v_i}{\partial t} + v_i\frac{\partial v_i}{\partial x} + \frac{T_i}{m_i n_i}\frac{\partial n_i}{\partial x} + \frac{e}{m_i}\frac{\partial \phi}{\partial x} = 0, \tag{2.b}$$

where n_i, v_i, m_i and T_i denote the ion density, ion velocity, ion mass and ion temperature, respectively. Here, we express Eq. (2b) by the isothermal equation of state.

For one dimensional low frequency acoustic motions, we have the following two equations for the cold dust particles,

$$\frac{\partial n_d}{\partial t} + \frac{\partial}{\partial x}(n_d v_d) = 0, \tag{3.a}$$

$$\left(\frac{\partial}{\partial t} + v_d \frac{\partial}{\partial x}\right)v_d - \frac{Q_d}{m_d}\frac{\partial \phi}{\partial x} = 0 \ , \tag{3.b}$$

where n_d, v_d and m_i refer to the dust grain density, dust fluid velocity and dust grain mass, respectively. Here the dust charge variable $Q_d = eZ_d$, where Z_d is the charge number of dust particles measured in units of e .

The Poisson's equation is given as

$$\frac{\partial^2 \phi}{\partial x^2} = \frac{e}{\varepsilon_0}(n_e - n_i + Z_d n_d), \tag{4}$$

where $m_d(m_i)$ denotes the dust grain (ion) mass. We assume that the phase velocity of electrostatic ion waves is low in comparison with the electron thermal velocity. Charge neutrality at equilibrium requires that $n_{i0} = n_0 + n_{d0} Z_d$, where n_{i0} (n_{d0}) denotes the equilibrium ion (dust grain) density. In this system, the ordering, $m_d >> m_i >> m_e$ holds, as is obtained in laboratory plasmas. Typical laboratory plasma frequencies are; 10^2Hz: $10^{5\text{-}6}$Hz: $10^{9\text{-}10}$Hz, and have roughly the same ordering as the mass ratios. Thus, the inclusion of the mass ratios is equal to considering the motion of dust particles.

We assume that the charging of the dust grain particles arises from plasma currents due to the electrons and the ions reaching the grain surface. In this case, the dust grain charge variable Q_d is determined by the charge current balance equation[22]:

$$\left(\frac{\partial}{\partial t} + v_d \frac{\partial}{\partial x}\right)Q_d = I_e + I_i \ , \tag{5}$$

Assuming that the streaming velocities of the electrons and ions are much smaller than their thermal velocities, we have the following expressions for the electron and ion currents for spherical grains of radius r:

$$I_e = -e\pi r^2 (8T_e/\pi m_e)^{1/2} n_e(\phi,\beta)\exp\left(\frac{e\Phi}{T_e}\right), \tag{6.a}$$

and

$$I_i = e\pi r^2 (8T_i/\pi m_i)^{1/2} n_i(\phi,\tau_i,\Psi)\left(1-\frac{e\Phi}{T_i}\right), \tag{6.b}$$

where $\Phi \equiv Q_d/r$ denotes the dust particle surface potential relative to the plasma potential ϕ. If the ion streaming velocity v_0 is much larger than the ion thermal velocity, the ion current is approximately expressed as $I_i \approx e\pi r^2 v_0 n_i(1-2e\Phi/m_i v_0^2)$. At equilibrium, equating $I_e + I_i$ to zero we obtain the floating potential Φ_0 and the equilibrium dust charge $Q_0 = C\Phi_0$, where C denotes the dust grain capacitance.

We normalize all the physical quantities as follows. The densities are normalized by the background electron density n_0. The space coordinate x, time t, velocities and electrostatic potential ϕ are normalized by the electron Debye length $\lambda_d=(\varepsilon_0 T_e/n_0e^2)^{1/2}$, the inverse ion plasma period $\omega_i^{-1}=(\varepsilon_0 m_i/n_0e^2)^{1/2}$, the ion sound velocity $C_s=(T_e/m_i)^{1/2}$, and T_e/e, respectively, where m_i, ε_0 and e are the ion mass, the permittivity of vacuum and the magnitude of electron charge, respectively.

In order to solve Eqs.(1)-(5), we introduce the variable $\xi = x - Mt$, which is the moving frame with the velocity M. We reduce a set of basic equations (1)-(4) to

$$n_e = \exp(\phi)\operatorname{erfc}(\sqrt{\phi}) + \frac{1}{\sqrt{\beta}}\exp(\beta\phi)\operatorname{erf}(\sqrt{\beta\phi}), \tag{7}$$

$$-M\frac{\partial n_i}{\partial \xi} + \frac{\partial}{\partial \xi}(n_i v_i) = 0, \tag{8.a}$$

$$-M\frac{\partial v_i}{\partial \xi} + v_i\frac{\partial v_i}{\partial \xi} + \frac{\tau_i}{n_i}\frac{\partial n_i}{\partial \xi} + \frac{\partial \phi}{\partial \xi} = 0, \tag{8.b}$$

$$-M\frac{\partial n_d}{\partial \xi} + \frac{\partial}{\partial \xi}(n_d v_d) = 0, \tag{9.a}$$

$$-M\frac{\partial v_d}{\partial \xi} + v_d\frac{\partial v_d}{\partial \xi} - \frac{Z_d}{\mu_d}\frac{\partial \phi}{\partial \xi} = 0, \tag{9.b}$$

$$\frac{\partial^2\phi}{\partial\xi^2} = n_e - n_i + Z_d n_d \,. \tag{10}$$

Here, $\tau_i = T_i / T_e$ and $\mu_d = m_d / m_i$.

Integrating (8.a) and (8.b) and using the boundary conditions, $\phi \to 0$, $n_d \to (\delta - 1)/Z_d$, $n_i \to \delta$, $v_i \to 0$, $v_d \to 0$, at $\xi \to \infty$, we obtain

$$n_i = \frac{\delta}{\sqrt{1 - \dfrac{2\phi}{M^2 - \tau_i}}} \quad , \tag{11}$$

after the brief calculation, where $\delta = n_{i0} / n_0$. Integration of (9.a) and (9.b) gives rise to

$$n_d = \frac{\delta - 1}{Z_d} \frac{1}{\sqrt{1 + \dfrac{Z_d}{\mu_d}\dfrac{2\phi}{M^2}}} \quad . \tag{12}$$

At equilibrium, Eq.(5) reduces to

$$-n_e(\phi,\beta)\exp(\Psi) + \sqrt{\frac{\tau_i}{\mu_i}}\, n_i(\phi,\tau_i)\left(1 - \frac{\Psi}{\tau_i}\right) = 0 \quad . \tag{13}$$

where $\mu_i = m_i / m_e$, $\Psi = e\Phi / T_e$, and the electron (ion) current I_e (I_i) is normalized by $e\pi r^2 (8T_e / \pi m_e)^{1/2}$. Equation (13) includes strongly nonlinear terms. In order to solve (13) exactly, we derive a following nonlinear equation for variable-charge of dust particles as

$$\left\{\exp(\phi)\operatorname{erfc}\left(\sqrt{\phi}\right)+\frac{1}{\sqrt{\beta}}\exp(\beta\phi)\operatorname{erf}\left(\sqrt{\beta\phi}\right)\right\}\exp(\Psi)$$

$$=\frac{\delta\left(\tau_i-\Psi\right)}{\sqrt{\mu_i\tau_i\left(1-\dfrac{2\phi}{M^2-\tau_i}\right)}} \quad . \tag{14}$$

We regard (14) as a new equation for the dust particle surface potential in this system. Then, we can obtain the solution of (14) by numerical calculation in the next section.

Integration of the Poisson's equation gives *the Energy Law,*

$$\frac{1}{2}\left(\frac{\partial\phi}{\partial\xi}\right)^2+V(\phi)=0 \quad , \tag{15}$$

with

$$V(\phi)=1-\exp(\phi)\operatorname{erfc}\sqrt{\phi}-2\left(1-\frac{1}{\beta}\right)\sqrt{\frac{\phi}{\pi}}-\frac{1}{\beta^{3/2}}\exp(\beta\phi)\operatorname{erf}\sqrt{\beta\phi}$$

$$+\delta\left(M^2-\tau_i\right)\left(1-\sqrt{1-\frac{2\phi}{M^2-\tau_i}}\right)+(\delta-1)\frac{\mu_d M^2}{\alpha\Psi}\left\{1-\sqrt{1+\frac{\alpha\Psi}{\mu_d}\frac{2\phi}{M^2}}\right\} \quad , \tag{16}$$

where $\alpha=rT_e/e^2$.

The oscillatory solution of the nonlinear electrostatic waves exists when the following conditions are satisfied:

(i) The pseudopotential $V(\phi)$ has the maximum value if $d^2V(\phi)/d\phi^2<0$ at $\phi=0$. It should be noted that $V(\phi)$ is real, when $0<\phi<\left(M^2-\tau_i\right)/2$. The region for existence of ϕ is characterized by these conditions. We understand that this region depend on the Mach number and the ion to electron temperature ratio.

(ii) Nonlinear waves exist only when $V(\phi_M) \geq 0$, where the maximum potential ϕ_M is determined by $\phi_M = (M^2 - \tau_i)/2$. This implies that the inequality

$$1 - \exp\left(\frac{M^2 - \tau_i}{2}\right) \operatorname{erfc}\sqrt{\frac{M^2 - \tau_i}{2}} - 2\left(1 - \frac{1}{\beta}\right)\sqrt{\frac{M^2 - \tau_i}{2\pi}} - \frac{1}{\beta^{3/2}} \exp\left\{\frac{\beta(M^2 - \tau_i)}{2}\right\} \operatorname{erf}\sqrt{\frac{\beta(M^2 - \tau_i)}{2}}$$
$$+ \delta(M^2 - \tau_i) + (\delta - 1)\frac{\mu_d M^2}{\alpha\Psi}\left(1 - \sqrt{1 + \frac{\alpha\Psi(M^2 - \tau_i)}{\mu_d M^2}}\right) \geq 0 \quad , \qquad (17)$$

holds.

We show the maximum Mach number as a function of δ in Fig.1a, in the case of β=0.25 (mark a on the curve) and β=1.4 (mark b on the curve) for τ_i=0.5, where r=10^{-7}, Z_d=5×10^4 and μ_d=10^{12}. For example a dust grain of radius 1 μm and mass density 2000kg/m^3 has a mass $\sim 5\times10^{-15}$kg so that $\mu_d \sim 10^{12}$. Figure 1b illustrates the dependence of the maximum Mach number on the free to trapped electron temperature ratio for τ_i=5×10^{-3} (mark a) and 0.5 (mark b), where r=10^{-7}, δ=50, μ_d=10^{12} and Z_d =10^5. The maximum Mach number and, correspondingly, the maximum amplitude of electrostatic ion waves significantly depends on the parameters β, δ and τ_i. It turns out that only the supersonic electrostatic waves can propagate in this system.

III. DYNAMICS OF THE CHARGE VARIATION OF DUST GRAINS

We examine the numerical analysis of the nonlinear equations obtained in the preceding section. For illustration purposes, we consider a dusty plasma in which most of the background electrons are collected by negatively-charged dust grains. Such a situation, for example, is common to the F-ring of Saturn and the environment of Jupiter [23]. Thus, without loss of generality, we calculate the dust charging effect concerning electrostatic nonlinear ion waves, by numerical calculation. In the following discussion, we assume that r=10^{-7}, T_e=1eV, μ_i=1836 and μ_d=10^{12}.

First, we study the dependence of the dust charging effect on the electrostatic potential. If $\beta > 0$, we show a $\Psi - \phi$ plane in Fig. 2a, in the case of M=1.4 (solid lines) and 1.2 (dashed lines), where $\beta = 0.5$ (mark a) and 1.0 (mark b). We note that, since an equation $Z_d = \alpha |\Psi|$ holds, the dust charge number is easily obtained by mutiplying Ψ by 6.25×10^{11}. As an example, we find that the dust charge number Z_d lies in $\sim 10^4$ -10^9, in the case of Fig.2a. The dust charge number gradually increases and subsequently decreases as the electrostatic potential increases. We understand that the charge number increases as the trapped electron temperature decreases because $\beta = T_e/T_t$, and increases as the Mach number increases. Figure 2b illustrates the dependence of the dust charge number on the ion to electron density ratio δ, in the case of M=2.2 (solid lines) and M=1.4 (dashed lines), where β=0.5 (mark a) and 1.0 (mark b). We find that an increase of the ion to electron density ratio decreases the charge number of dust grains, and an increase of the Mach number increases the dust charge number. Figure 3a shows the dependence of the dust charge number on the ratio of the ion to electron temperature τ_i for M=1.5 (solid lines) and M=1.2 (dashed lines), where β = 0.1 (mark a) and 1.0 (mark b). It turns out that the dust charge number increases within the range of τ_i<0.04 for M=1.5 (τ_i<0.03 for M=1.2) and decreases as the ion temperature increases (τ_i>0.04 for M=1.5 and τ_i>0.03 for M=1.2). The dust charging ratio of the higher Mach number is higher than that of the smaller one. When the ion temperature decreases, dust grain particles are highly charged. In order to show a relationship between the normalized floating potential and the Mach number, we illustrate a $\Psi - M$ plane in Fig.3b for the ion to electron density ratio δ=100 (solid lines) and 50 (dashed lines), and the ion to electron temperature ratio τ_i=0.5 (mark a) and 1.0 (mark b), where β=5.0 and ϕ=0.5. In this case, the floating potential does not vary as the ratio of the free to trapped electron temperature changes. It is found that the floating potential of dust grains decreases as the Mach number increases, and becomes higher for the lower ion to electron temperature ratio. The floating potential grows, in the same way, as the Mach number increases, and becomes higher for the lower contamination ratio of the ion density.

Second, we show a 3-dimensional (3-D) Sagdeev potential in Fig.4a as a typical case where Z_d=5× 10^4, M=1.8, β=5.0 and τ_i=0.01, and illustrate a 2-dimensional (2-D) Sagdeev potential in Fig.4b in the case where δ=100 (mark a) and 200 (mark b). We understand that the existence of nonlinear electrostatic waves drastically changes due to the ion to electron density ratio.

Thus, we understand that the dust charge number sensitively depends on the parameters such as the floating potential of dust particles, electrostatic potential of the plasma, trapped electron temperature, Mach number, ion density and temperature.

IV. DISCUSSION

In this article, we have shown the effect of the dust charging of electrostatic waves in a dusty plasma whose constituents are trapped electrons, ions with the finite temperature and a cold dust fluid consisting of negatively-charged, micrometer-sized dust particles. Such plasmas may exist in both space environments and laboratory. We find the remarkable properties of the charging effect of dust grain particles obtained here as follows.

(1) Supersonic ion waves can propagate in this system. Dependence of the Mach

number on the ion to electron density ratio drastically changes due to the trapped electron temperature and ion temperature. An increase of the Mach number increases the dust charge number.

(2) Dependence of the charge variation of dust particles on the trapped electron temperature, ion density and temperature is found for the first time in dusty plasmas. The effect of the ion temperature decreases the dust charge number. Since the effect of the ion temperature affects the characteristics of the collective motion of the plasma, this effect is important in understanding nonlinear waves propagating in dusty plasmas.

(3) The dust charging effect is of crucial importance in the sense that the dust charge number drastically changes due to the parameters such as the floating potential of dust particles, electrostatic potential of the plasma, ion to electron density ratio dust to ion mass ratio, trapped electron temperature, ion temperature and Mach number. The region for existence of nonlinear waves varies due to the ion to electron density ratio and floating potential of dust grain particles.

In a recent plasma etch experiment[24], it has been suggested that electrostatic waves may be responsible for the trapping of micrometer- and submicrometer-sized contamination particles within the plasma[13]. As is mentioned in this article, the inclusion of trapped electrons is required to consider nonlinear dust waves. If such waves are present in dusty plasmas, which are observed in planetary, cometary, other space environments and technological-aided plasmas, the investigation of their peculiar features will contribute to the future development in dusty plasmas. As a possible example, they may serve as a source for the intense jovian dust streams observed in the environment of Jupiter[23]. In this situation, our results are important in understanding the nonlinear charging mechanism of the streaming of dust grain particles and confirming the existence of arbitrary amplitude electrostatic waves in dusty plasmas.

ACKNOWLEDGEMENT

The author wishes to thank the Special Research Program and the Project Research Program of Hachinohe Institute of Technology, and the Joint Research Program of the National Institute for Fusion Science.

APPENDIX: THE PROFILE OF THE TRAPPED ELECTRON DENSITY

It is significant to consider the dependence of the trapped electron density n_e on the electrostatic potential ϕ and free to trapped electron temperature ratio β in the sense that electrostatic ion waves closely connect with the trapped electron density. In order to investigate the relationship, we show the trapped electron density n_e as a function of ϕ and β associated with Eq.(7). We illustrate a bird's eye view in Fig.5a, and a n_e-ϕ plane in Fig.5b, for β=0.75 (mark a), 2.0 (mark b) and 5.0 (mark c). As is seen in Figs. 5a and 5b, we find the following. In the case where $\beta<1$, the trapped electron density n_e lies in the small range even if the electrostatic potential ϕ grows. If $\beta>1$, n_e remains a small value for $\phi<1$ but grows for $\phi>1$. The higher β becomes, the grower n_e becomes exponentially. It turns out that, when β becomes larger, this tendency becomes remarkable.

References

[1] C.K.Goertz, Rev. Geophys. **27**, 1764 (1986).

[2] E.Grun, G.E.Morfill and D.A.Mendis, in *Planetary Rings* (Univ. Arizona Press, Tucson, 1984), p.275.

[3] T.W.Hartquist, O.Havnes and G.E.Morfill, Fundam. Cosmic Phys. **15**, 107 (1992).

[4] V.N.Tsytovich, and O.Havnes, Comm. Plasma Phys. Control. Fusion, **15**, 267 (1993).

[5] R.Bingham, U.de Angelis, V.N.Tsytovich, and O.Havnes, Phys. Fluids B **3**, 811 (1991).

[6] G.S.Selwyn, J.E.Heidenreich and K.L.Haller, Appl. Phys. Lett. **57**, 1876 (1990).

[7] L.Boufendi, A.Plain, J.P.Blondeau, A.Bouchoule, C.Laure and M.Toogood Appl. Phys. Lett. **60**, 169 (1992).

[8] C.K.Goertz and G.E.Morfill, Icarus **53**, 219 (1983).

[9] N.N.Rao, P.K.Shukla and M.Y.Yu, Planet. Space Sci. **38**, 543 (1990).

[10] R.K.Varma, P.K.Schukla and V.Krishan, Phys. Rev. E, **47**, 3612 (1993).

[11] Y-N.Nejoh, IEEE Trans. Plasma Sci. **25**, 492 (1997).

[12] A Barkan, and R.L.Merlino, Phys. Plasmas **2**, 3261 (1995).

[13] A.Barkan, R.L.Merlino and N.D'Angelo, Phys. Plasmas **2**, 3563 (1995).

[14] Y-N.Nejoh, Phys. Plasmas **2**, 4122 (1995).

[15] Y-N.Nejoh, Austr. J. Phys. **49**, 956 (1996) .

[16] Y-N.Nejoh, Phys. Plasmas **3**, 1447 (1996).

[17] Y-N.Nejoh, J. Plasma Phys. **56**, 67 (1996).

[18] J.P.Lynov, P.Michelson, H.L.Pecseli, J.Rasmussen, Phys. Lett., **80**, 23 (1980).

[19] Y-N.Nejoh, Astrophys. Space Sci. **235**, 245 (1996); M.Raadu, Phys. Rep. **178**, 25 (1989).

[20]J.E.Borovsky and G.Joyce, J. Plasma Phys. **29**, 45 (1983).

[21]H.Schamel, J. Plasma Phys. **9**, 377 (1973).

[22] F.Melandso, F.T.Askalsen and O.Havnes, Planet. Space Sci. **41**, 312 (1993).

[23] E.Grun, E.H.Zook, M.Baguhl, A.Balogh, S.J.Bame, H.Fechtig, R.Forsyth, M.S.Hanner, M.Horanyi, J.Kissel, B.A.Lindblad, D.Linkert, G.Linkert, I.Mann, J.A.McDonnel, G.E.Morfil, J.L.Phillips, C.Polanskey, G.Schwehm, N.Siddique, P.Staubach, J.Svestka, A.Taylor, Nature **362**, 428 (1993).

[24]J.W.Coburn and H.F.Winters, J. Appl. Phys. **50**, 3189 (1979).

FIGURE CAPTIONS

Fig.1a The maximum Mach number as a function of the ion to electron density ratio in the case of β=0.25 (mark a on the curve) and β=1.4 (mark b on the curve) for τ_i=0.5, where Z_d=5× 10^4.

Fig.1b The dependence of the maximum Mach number on the ratio of the free to trapped electron temperature for τ_i =5× 10^{-3} (mark a) and 0.5 (mark b), where Z_d=10^5 and δ =50.

Fig.2a The dependence of the dust charging effect on the electrostatic potential. A $\Psi - \phi$ plane, in the case of M=1.4 (solid lines) and M=1.2 (dashed lines), where β=0.5 (mark a) and 1.0 (mark b).

Fig.2b The dependence of the dust charge number on the ion to electron density ratio in the case of M=2.2 (solid lines) and M=1.4 (dashed lines), where β=0.5 (mark a) and 1.0 (mark b).

Fig.3a The dependence of the dust charge number on the ratio of the ion to electron temperature τ_i for M=1.5 (solid lines) and M=1.2 (dashed lines), where β =0.1 (mark a) and 1.0 (mark b).

Fig.3b A $\Psi - M$ plane for the ion to electron density ratio δ=100 (solid lines) and 50 (dashed lines), where β=5.0 and ϕ=0.5. Marks *a* and *b* on the curves denote τ_i=0.5 and 1.0, respectively.

Fig.4a A 3-D Sagdeev potential in the case where Z_d=5 × 10^4, M=1.8, β=5.0 and τ_i=0.01.

Fig.4b A 2-D Sagdeev potential as is shown with the two cases of δ=100 (mark *a*) and 200 (mark *b*), where Z_d=5 × 10^4, M=1.8, β=5.0 and τ_i=0.01.

Fig.5a A bird's eye view of the trapped electron density n_e depending on the electrostatic potential ϕ and free to trapped electron temperature β.

Fig.5b A n_e-ϕ plane, for β=0.75 (mark *a*), 2.0 (mark *b*) and 5.0 (mark *c*).

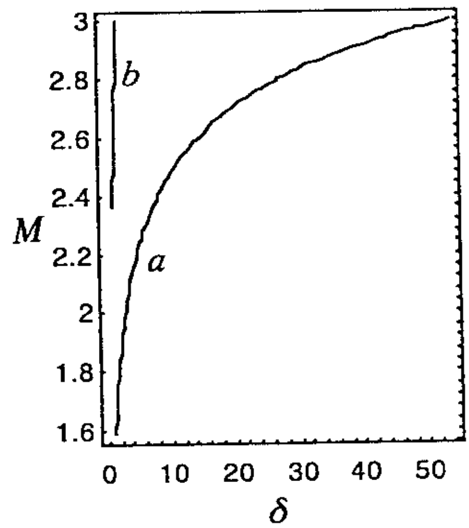

3
2.8
2.6
2.4
M
2.2
2
1.8
1.6
b
a
0
10
20
30
40
50
δ

(a)

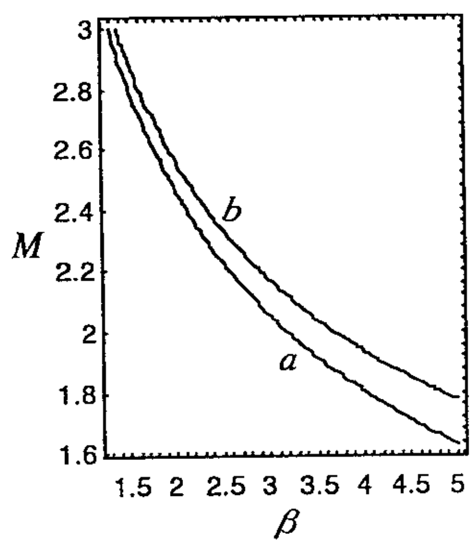

3
2.8
2.6
2.4
M
2.2
2
1.8
1.6
b
a
1.5
2
2.5
3
3.5
4
4.5
5
β

(b)

Fig.1

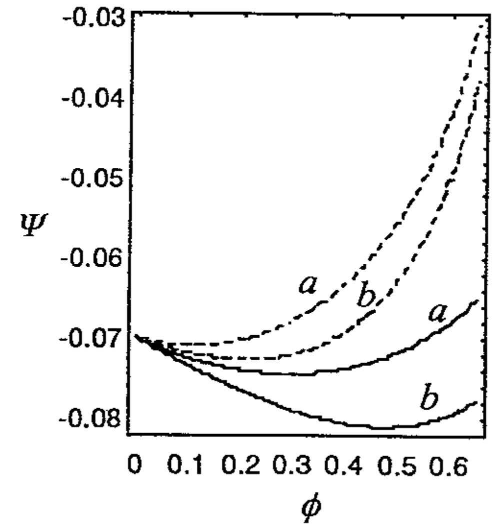
-0.03
-0.04
-0.05
-0.06
-0.07
-0.08
Ψ
a
b
a
b
0 0.1 0.2 0.3 0.4 0.5 0.6
ϕ

(a)

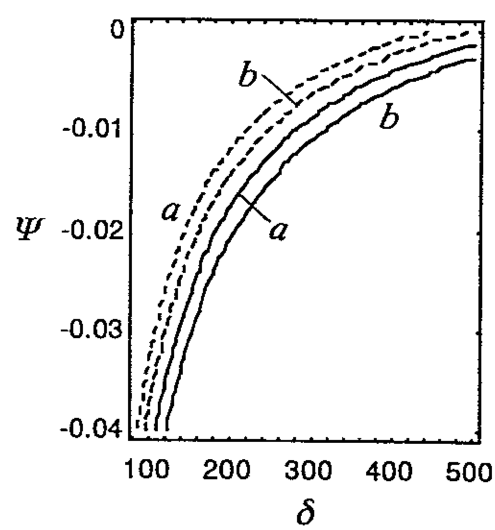
0
-0.01
-0.02
-0.03
-0.04
Ψ
b
a
b
a
100 200 300 400 500
δ

(b)

Fig.2

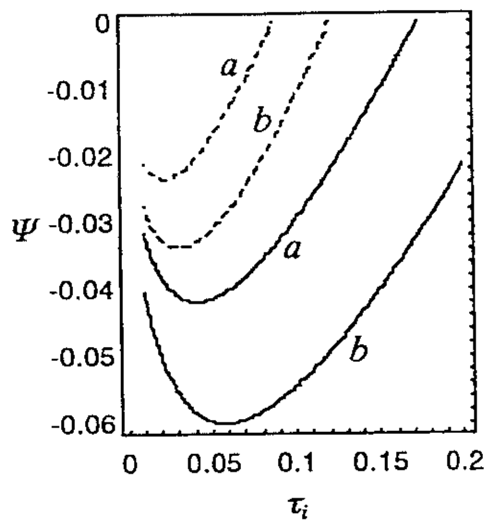

0
-0.01
-0.02
-0.03
-0.04
-0.05
-0.06
a
b
a
b
ψ
0
0.05
0.1
0.15
0.2
τ_i

(a)

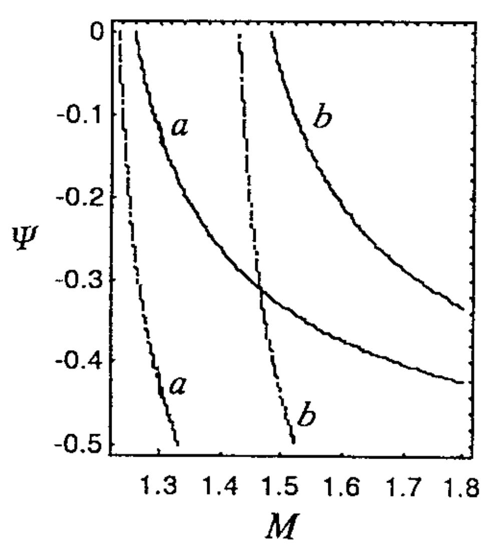

0
-0.1
-0.2
-0.3
-0.4
-0.5
a
b
a
b
ψ
1.3
1.4
1.5
1.6
1.7
1.8
M

(b)

Fig.3

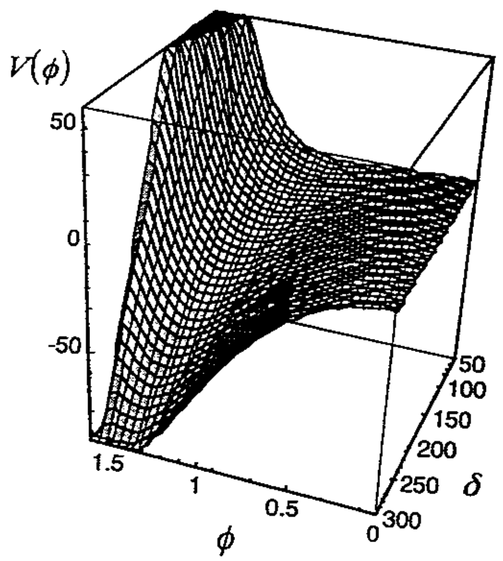

V(ϕ)
50
0
-50
1.5
1
0.5
0
ϕ
50
100
150
200
250
300
δ

(a)

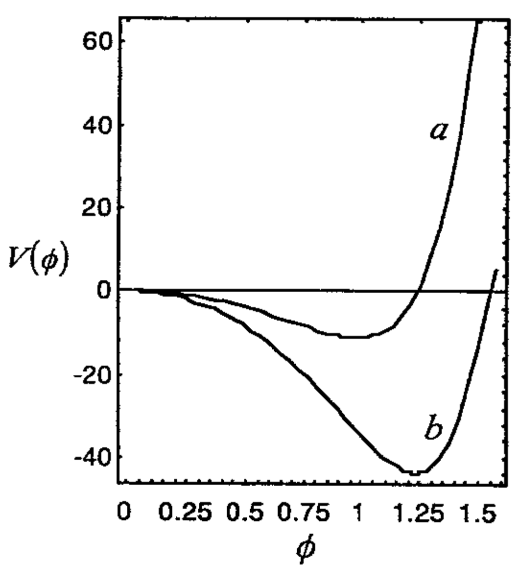

60
40
20
V(ϕ)
0
-20
-40
a
b
0
0.25
0.5
0.75
1
1.25
1.5
ϕ

(b)

Fig.4

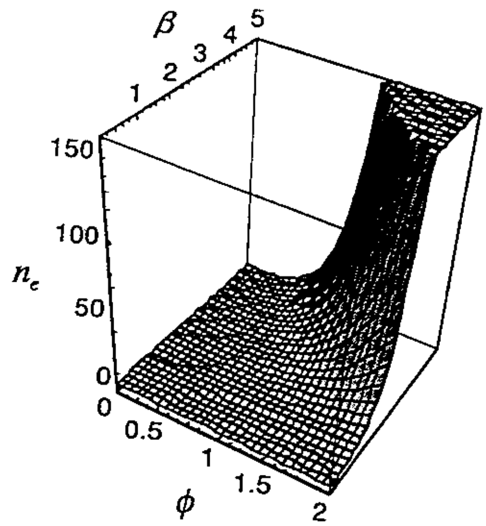

β
1
2
3
4
5
150
100
50
0
n_e
0
0.5
1
1.5
2
φ

(a)

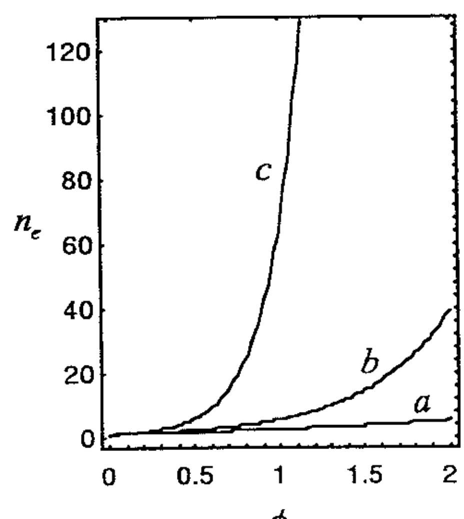

120
100
80
60
40
20
0
n_e
c
b
a
0
0.5
1
1.5
2
φ

(b)

Fig.5

Recent Issues of NIFS Series

NIFS-462 N. Katsuragawa, H. Hojo and A. Mase,
Simulation Study on Cross Polarization Scattering of Ultrashort-Pulse Electromagnetic Waves; Nov. 1996

NIFS-463 V. Voitsenya, V. Konovalov, O. Motojima, K. Narihara, M. Becker and B. Schunke,
Evaluations of Different Metals for Manufacturing Mirrors of Thomson Scattering System for the LHD Divertor Plasma; Nov. 1996

NIFS-464 M. Pereyaslavets, M. Sato, T. Shimozuma, Y. Takita, H. Idei, S. Kubo, K. Ohkubo and K. Hayashi,
Development and Simulation of RF Components for High Power Millimeter Wave Gyrotrons; Nov. 1996

NIFS-465 V.S. Voitsenya, S. Masuzaki, O. Motojima, N. Noda and N. Ohyabu,
On the Use of CX Atom Analyzer for Study Characteristics of Ion Component in a LHD Divertor Plasma; Dec. 1996

NIFS-466 H. Miura and S. Kida,
Identification of Tubular Vortices in Complex Flows; Dec. 1996

NIFS-467 Y. Takeiri, Y. Oka, M. Osakabe, K. Tsumori, O. Kaneko, T. Takanashi, E. Asano, T. Kawamoto, R. Akiyama and T. Kuroda,
Suppression of Accelerated Electrons in a High-current Large Negative Ion Source; Dec. 1996

NIFS-468 A. Sagara, Y. Hasegawa, K. Tsuzuki, N. Inoue, H. Suzuki, T. Morisaki, N. Noda, O. Motojima, S. Okamura, K. Matsuoka, R. Akiyama, K. Ida, H. Idei, K. Iwasaki, S. Kubo, T. Minami, S. Morita, K. Narihara, T. Ozaki, K. Sato, C. Takahashi, K. Tanaka, K. Toi and I. Yamada,
Real Time Boronization Experiments in CHS and Scaling for LHD; Dec. 1996

NIFS-469 V.L. Vdovin, T.Watari and A. Fukuyama,
3D Maxwell-Vlasov Boundary Value Problem Solution in Stellarator Geometry in Ion Cyclotron Frequency Range (final report); Dec. 1996

NIFS-470 N. Nakajima, M. Yokoyama, M. Okamoto and J. Nührenberg,
Optimization of M=2 Stellarator; Dec. 1996

NIFS-471 A. Fujisawa, H. Iguchi, S. Lee and Y. Hamada,
Effects of Horizontal Injection Angle Displacements on Energy Measurements with Parallel Plate Energy Analyzer; Dec. 1996

NIFS-472 R. Kanno, N. Nakajima, H. Sugama, M. Okamoto and Y. Ogawa,
Effects of Finite-β and Radial Electric Fields on Neoclassical Transport in the Large Helical Device; Jan. 1997

NIFS-473 S. Murakami, N. Nakajima, U. Gasparino and M. Okamoto,
Simulation Study of Radial Electric Field in CHS and LHD; Jan. 1997

NIFS-474 K. Ohkubo, S. Kubo, H. Idei, M. Sato, T. Shimozuma and Y. Takita,
Coupling of Tilting Gaussian Beam with Hybrid Mode in the Corrugated Waveguide; Jan. 1997

NIFS-475 A. Fujisawa, H. Iguchi, S. Lee and Y. Hamada,
Consideration of Fluctuation in Secondary Beam Intensity of Heavy Ion Beam Prove Measurements; Jan. 1997

NIFS-476 Y. Takeiri, M. Osakabe, Y. Oka, K. Tsumori, O. Kaneko, T. Takanashi, E. Asano, T. Kawamoto, R. Akiyama and T. Kuroda,
Long-pulse Operation of a Cesium-Seeded High-Current Large Negative Ion Source; Jan. 1997

NIFS-477 H. Kuramoto, K. Toi, N. Haraki, K. Sato, J. Xu, A. Ejiri, K. Narihara, T. Seki, S. Ohdachi, K. Adati, R. Akiyama, Y. Hamada, S. Hirokura, K. Kawahata and M. Kojima,
Study of Toroidal Current Penetration during Current Ramp in JIPP T-IIU with Fast Response Zeeman Polarimeter; Jan., 1997

NIFS-478 H. Sugama and W. Horton,
Neoclassical Electron and Ion Transport in Toroidally Rotating Plasmas; Jan. 1997

NIFS-479 V.L. Vdovin and I.V. Kamenskij,
3D Electromagnetic Theory of ICRF Multi Port Multi Loop Antenna; Jan. 1997

NIFS-480 W.X. Wang, M. Okamoto, N. Nakajima, S Murakami and N. Ohyabu,
Cooling Effect of Secondary Electrons in the High Temperature Divertor Operation; Feb. 1997

NIFS-481 K. Itoh, S.-I. Itoh, H. Soltwisch and H.R. Koslowski,
Generation of Toroidal Current Sheet at Sawtooth Crash; Feb. 1997

NIFS-482 K. Ichiguchi,
Collisionality Dependence of Mercier Stability in LHD Equilibria with Bootstrap Currents; Feb. 1997

NIFS-483 S. Fujiwara and T. Sato,
Molecular Dynamics Simulations of Structural Formation of a Single Polymer Chain: Bond-orientational Order and Conformational Defects; Feb. 1997

NIFS-484 T. Ohkawa,
Reduction of Turbulence by Sheared Toroidal Flow on a Flux Surface; Feb. 1997

NIFS-485 K. Narihara, K. Toi, Y. Hamada, K. Yamauchi, K. Adachi, I. Yamada, K. N. Sato, K.

Kawahata, A. Nishizawa, S. Ohdachi, K. Sato, T. Seki, T. Watari, J. Xu, A. Ejiri, S. Hirokura, K. Ida, Y. Kawasumi, M. Kojima, H. Sakakita, T. Ido, K. Kitachi, J. Koog and H. Kuramoto,
Observation of Dusts by Laser Scattering Method in theJIPPT-IIU Tokamak
Mar. 1997

NIFS-486 S. Bazdenkov, T. Sato and The Complexity Simulation Group,
Topological Transformations in Isolated Straight Magnetic Flux Tube; Mar. 1997

NIFS-487 M. Okamoto,
Configuration Studies of LHD Plasmas; Mar. 1997

NIFS-488 A. Fujisawa, H. Iguchi, H. Sanuki, K. Itoh, S. Lee, Y. Hamada, S. Kubo, H. Idei, R. Akiyama, K. Tanaka, T. Minami, K. Ida, S. Nishimura, S. Morita, M. Kojima, S. Hidekuma, S.-I. Itoh, C. Takahashi, N. Inoue, H. Suzuki, S. Okamura and K. Matsuoka,
Dynamic Behavior of Potential in the Plasma Core of the CHS Heliotron/Torsatron; Apr. 1997

NIFS-489 T. Ohkawa,
Pfirsch - Schlüter Diffusion with Anisotropic and Nonuniform Superthermal Ion Pressure; Apr. 1997

NIFS-490 S. Ishiguro and The Complexity Simulation Group,
Formation of Wave-front Pattern Accompanied by Current-driven Electrostatic Ion-cyclotron Instabilities; Apr. 1997

NIFS-491 A. Ejiri, K. Shinohara and K. Kawahata,
An Algorithm to Remove Fringe Jumps and its Application to Microwave Reflectometry; Apr. 1997

NIFS-492 K. Ichiguchi, N. Nakajima, M. Okamoto,
Bootstrap Current in the Large Helical Device with Unbalanced Helical Coil Currents; Apr. 1997

NIFS-493 S. Ishiguro, T. Sato, H. Takamaru and The Complexity Simulation Group,
V-shaped dc Potential Structure Caused by Current-driven Electrostatic Ion-cyclotron Instability; May 1997

NIFS-494 K. Nishimura, R. Horiuchi, T. Sato,
Tilt Stabilization by Energetic Ions Crossing Magnetic Separatrix in Field-Reversed Configuration; June 1997

NIFS-495 T. -H. Watanabe and T. Sato,
Magnetohydrodynamic Approach to the Feedback Instability; July 1997

NIFS-496 K. Itoh, T. Ohkawa, S. -I.Itoh, M. Yagi and A. Fukuyama
Suppression of Plasma Turbulence by Asymmetric Superthermal Ions; July 1997

NIFS-497 T. Takahashi, Y. Tomita, H. Momota and Nikita V. Shabrov,
Collisionless Pitch Angle Scattering of Plasma Ions at the Edge Region of an FRC; July 1997

NIFS-498 M. Tanaka, A.Yu Grosberg, V.S. Pande and T. Tanaka,
Molecular Dynamics and Structure Organization in Strongly-Coupled Chain of Charged Particles; July 1997

NIFS-499 S. Goto and S. Kida,
Direct-interaction Approximation and Reynolds-number Reversed Expansion for a Dynamical System; July 1997

NIFS-500 K. Tsuzuki, N. Inoue, A. Sagara, N. Noda, O. Motojima, T. Mochizuki, T. Hino and T. Yamashina,
Dynamic Behavior of Hydrogen Atoms with a Boronized Wall; July 1997

NIFS-501 I. Viniar and S. Sudo,
Multibarrel Repetitive Injector with a Porous Pellet Formation Unit; July 1997

NIFS-502 V. Vdovin, T. Watari and A. Fukuyama,
An Option of ICRF Ion Heating Scenario in Large Helical Device; July 1997

NIFS-503 E. Segre and S. Kida,
Late States of Incompressible 2D Decaying Vorticity Fields; Aug. 1997

NIFS-504 S. Fujiwara and T. Sato,
Molecular Dynamics Simulation of Structural Formation of Short Polymer Chains; Aug. 1997

NIFS-505 S. Bazdenkov and T. Sato
Low-Dimensional Model of Resistive Interchange Convection in Magnetized Plasmas; Sep. 1997

NIFS-506 H. Kitauchi and S. Kida,
Intensification of Magnetic Field by Concentrate-and-Stretch of Magnetic Flux Lines; Sep. 1997

NIFS-507 R.L. Dewar,
Reduced form of MHD Lagrangian for Ballooning Modes; Sep. 1997

NIFS-508 Y.-N. Nejoh,
Dynamics of the Dust Charging on Electrostatic Waves in a Dusty Plasma with Trapped Electrons; Sep.1997